



**HAL**  
open science

# Dissipative Wave Model Fitting Using Localized Sources

Nicolas Schmidt, Gabriel Peyré, Yves Frégnac

► **To cite this version:**

Nicolas Schmidt, Gabriel Peyré, Yves Frégnac. Dissipative Wave Model Fitting Using Localized Sources. 2011. hal-00570685

**HAL Id: hal-00570685**

**<https://hal.science/hal-00570685>**

Preprint submitted on 28 Feb 2011

**HAL** is a multi-disciplinary open access archive for the deposit and dissemination of scientific research documents, whether they are published or not. The documents may come from teaching and research institutions in France or abroad, or from public or private research centers.

L'archive ouverte pluridisciplinaire **HAL**, est destinée au dépôt et à la diffusion de documents scientifiques de niveau recherche, publiés ou non, émanant des établissements d'enseignement et de recherche français ou étrangers, des laboratoires publics ou privés.

# Dissipative Wave Model Fitting Using Localized Sources

N. Schmidt<sup>†\*</sup>, G. Peyré<sup>†</sup> and Y. Frégnac<sup>‡</sup>

<sup>†</sup>Ceremade, Université Paris-Dauphine, Paris, France

<sup>‡</sup>U.N.I.C., Institut de Neurobiologie Alfred Fessard, Gif-sur-Yvette, France

\*Email: schmidt@ceremade.dauphine.fr

**Abstract.** This paper introduces a novel method to estimate the parameters of a linear dissipative wave model from noisy observations. We focus on the case of constant coefficients and an unknown localized source. These constraints are motivated by applications in computational neuroscience and in particular separation of sources in the visual cortex in optical imaging modality. The proposed method takes advantage of the specificity of the model, namely the small number of parameters and the knowledge of the spatial support of the sources. It makes use of a temporal dimensionality reduction performed using a Laplace transform to drastically reduce the numerical complexity of the method. A Green kernel representation of the partial differential equation (PDE) solution exploiting the locality of the sources allows us to recover the parameters without the precise knowledge of the sources. A numerical evaluation of the method on synthetic data shows the strong robustness to noise of our method.

## 1 Introduction

**Biological motivation.** This work studies a particular inverse problem in 2-D wave imaging, motivated by the problem of neural sources separation in the visual brain. Optical imaging with voltage sensitive dye (VSDOI) offers the possibility to image with a high temporal and spatial resolution the activity of the early visual area of the cortex [5]. A challenging problem is to separate the different activity patterns emerging over the cortex. In some restricted experimental setups, it has been observed that the activity is characterized by waves that propagate over the 2-D cortical surface at approximately constant speed [8], [2], [9]. In a previous work [10] we proposed to model this activity using a simple wave equation with spatially localized sources. Estimating the parameters of this model (e.g. speed and diffusivity) is however challenging because of the very large noise level that contaminates the observations. In this paper, we propose a fast method to achieve a robust estimation of these parameters.

**Previous works.** A large amount of work has been devoted in seismic imaging to estimate spatially varying speeds when sources are fully known and the propagating waves are observed on the boundary of the domain, see for instance [1] and the reference therein. This leads

to a non-convex inverse problem, that is challenging to solve because of its high dimensionality. Specific methods can be developed in the case where the sources are sparse and localized, see for instance [6]. Another class of methods assumes some degree of randomness on the (unknown) sources, and use a statistical analysis on the recorded signals to estimate the parameters (e.g. travel times or speeds), see for instance [11], [7], [4], [3]. In this paper, we consider a different setup, where only the spatial support of the sources are known.

**Contribution.** This paper introduces a novel imaging paradigm, that might be relevant for some applications in computational neuroscience. We stress the importance of having some prior knowledge about the spatial localization of the sources, and imposing a small number of parameters (e.g. constant coefficients). We also provide a numerical scheme that makes use of a representation of the propagating wave over the Laplace domain. This representation uses a reduced number of green kernels localized on the boundary of the source support. This leads to a fast scheme that does not need repeated simulations of the space/time wave propagations.

## 2 Wave Generation Forward Model

**Linear PDE model.** Biological considerations led us to formulate a simple linear model for the propagation of the information in the early areas of the visual cortex [10]. The measured observation  $X = u + w$  is assumed to be composed of a signal  $u$  caused by the visual excitation and an additive noise  $w$  caused by the neural activity and the imaging device. The signal is assumed to propagate in time according to a linear wave equation parameterized by (unknown) coefficients  $\alpha_0 = (a_0, b_0, c_0) \in \mathbb{R}^3$  and an (unknown) source  $f_0(t, x)$ . It thus solves

$$a_0 \frac{\partial^2 u}{\partial t^2} + b_0 \frac{\partial u}{\partial t} + c_0 u - \Delta u = f_0 \quad (1)$$

on  $\mathbb{R}^2 \times (0, +\infty)$ , with boundary conditions  $\frac{\partial^k u}{\partial t^k} = 0$  at  $t = 0$  for  $k = 0, 1$ . In the following, we denote as  $u = T_{\alpha_0}(f_0)$  the propagating operator that maps the sources to the signal. For positive values of  $\alpha_0$ , this model leads to propagating and dissipative waves that might be useful to model certain neural activities. In this paper we

restrict our attention to this second order model, although our method could be used for more general linear PDEs.

**Source constraint.** In accordance with some biological observations [10], we consider a spatial constraint on the support of the sources

$$\mathcal{C}_x = \{f \mid \forall x \notin \Omega, \forall t > 0, f(x, t) = 0\}$$

where  $\Omega \subset \mathbb{R}^2$  is a known compact set. Figure 1 shows an example of a typical propagation that is achieved with this model using sources supported inside two small disks.

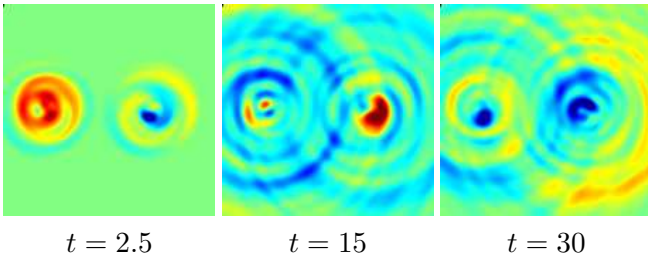


Figure 1: Example of a 2-D wave  $u$  propagating according to our model.

**Inverse problem.** The coefficient estimation problem requires to estimate  $\alpha = (a, b, c) \in \mathbb{R}^3$  in order for the observations  $X$  to be well approximated by a propagating wave  $X \approx T_\alpha(f)$  for some source  $f$ . An efficient method should provide an estimate  $\alpha$  close to the true value  $\alpha_0$  even in the presence of a large noise  $w$  contaminating the observations. The following theorem asserts that the true value  $\alpha_0$  can be uncovered in the absence of noise.

**Theorem 2.1.** *If  $f_0 \in \mathcal{C}_x$ , then  $T_{\alpha_0}(f_0) = T_\alpha(f)$  implies  $(\alpha, f) = (\alpha_0, f_0)$ .*

This suggests to jointly estimate  $\alpha$  and  $f$  by minimizing the deviation between  $X$  and  $T_\alpha(f)$ . This is however a difficult task because of the high dimensionality of  $f$  and the presence of a large noise which might lead to a poor solution. We propose here to avoid estimating the source  $f$  by exploiting the constraint  $\mathcal{C}_x$ . Once  $\alpha$  has been computed, it is easy to recover the sources  $f$  by solving the linear equation  $X = T_\alpha(f)$ , possibly with some regularization to remove the noise.

### 3 Green Representation of the Wave Model

This section details our main mathematical analysis of the model. The resulting estimation procedure is described in the next section.

**Laplace transform.** To reduce the computational complexity of the method, we remove the temporal dimension

by performing a Laplace transform, given some  $\beta > 0$

$$Y(x) = \int_0^{+\infty} e^{-\beta t} X(t, x) dt \quad (2)$$

where we have omitted the dependency on  $\beta$  for the sake of readability. The following proposition shows that the original PDE (1) is projected to a 2-D Helmholtz equation over the Laplace domain.

**Proposition 3.1.** *If  $w = 0$  and  $f_0 \in \mathcal{C}_x$ ,  $Y$  satisfies*

$$q_0(\beta)Y - \Delta Y = 0 \quad \text{in } \mathbb{R}^2 \setminus \Omega \quad (3)$$

where the shape parameter is  $q_0(\beta) = a_0\beta^2 + b_0\beta + c_0$ .

Inspired by this proposition, our strategy is thus to estimate the value of the shape parameter  $q(\beta)$  for different values of  $\beta$  in order to recover the value of  $\alpha_0$ .

**Green kernel extrapolation.** For each value of the shape parameter  $q \in \mathbb{R}$ , the Green solution (or fundamental solution)  $G_{x,q}$  at  $x \in \mathbb{R}^2$  of the Helmholtz equation (3) on the whole domain  $\mathbb{R}^2$  is given by

$$G_{x,q}(y) = K_0(\sqrt{q} \|x - y\|)$$

where  $K_0$  is the modified Bessel function of the second kind. At a point  $y \in \partial\Omega$  of the boundary of  $\Omega$ , we denote as  $\partial_{\bar{n}} G_{x,q}(y)$  the derivative of  $G_{x,q}$  in the direction normal to  $\partial\Omega$ .

Given a set of values  $A = (A(x))_{x \in \partial\Omega}$  and derivative values  $B = (B(x))_{x \in \partial\Omega}$  defined on this boundary, one obtains a function on the whole spatial domain by the following Green extrapolation

$$H_q(A, B)(x) = -\frac{1}{2\pi} \int_{\partial\Omega} (A(y) \partial_{\bar{n}} G_{x,q}(y) - B(y) G_{x,q}(y)) dy$$

where the integral is performed along the 1-D contour of the boundary.

**Dissipative wave reproducing formula.** Our main result is the following theorem, that expresses the fact that in the noiseless setting, the Laplace transform of the observations can be extrapolated to the whole domain given only its values on the boundary  $\partial\Omega$ . We denote respectively as  $A_Y$  and  $B_Y$  the restriction to  $\partial\Omega$  of  $Y$  and its derivative normal to  $\partial\Omega$ .

**Theorem 3.1.** *If  $w = 0$ , one has for all  $x \notin \Omega$*

$$Y(x) = H_{q_0(\beta)}(A_Y, B_Y)(x)$$

where  $q_0(\beta)$  is defined in proposition 3.1.

## 4 Wave Model Fitting Algorithm

**Fitting procedure.** Our parameter estimation method proceeds in two steps:

- **Step 1:** for each  $\beta \in \Sigma$ , compute an estimate of the shape parameter by solving

$$q(\beta) = \operatorname{argmin}_q E_\beta(q) \quad (4)$$

$$\text{where } E_\beta(q) = \min_{A,B} \|Y - H_q(A, B)\|_{L^2(\Omega^c)}^2. \quad (5)$$

- **Step 2:** estimate the parameter  $\alpha_0$  by computing the optimal  $\alpha$  solving

$$\min_{\alpha=(a,b,c) \in \mathbb{R}^3} \sum_{\beta \in \Sigma} |a\beta^2 + b\beta + c - q(\beta)|^2. \quad (6)$$

Theorem 3.1 asserts that in the noiseless case,  $w = 0$ , one has  $q(\beta) = q_0(\beta)$ , and proposition (3.1) thus implies that  $\alpha = \alpha_0$  so that the estimation procedure succeeds. Equality does not hold in the general case, but the  $L^2$  fit (5) of a single parameter from data on the domain  $\Omega^c = \mathbb{R}^2 \setminus \Omega$  guarantees a strong robustness to noise.

**Discrete algorithm.** In a numerical scenario, the data  $X$  is sampled at discrete locations in space and time, so that the  $L^2$  regression (5) is performed on the discrete grid points lying outside  $\Omega$ .

In order to be able to compute accurately the Laplace transform  $Y$  of  $X$  we assume that the propagating wave  $T_{\alpha_0}(f_0)$  is vanishing for  $t > t_0$ , and the integral (2) is estimated numerically from the available time samples. The set  $\Sigma$  of tested  $\beta$  values is a uniform discretization of an interval  $[0, \beta_{\max}]$  at  $|\Sigma|$  locations.

The resolution (4) corresponds to a minimization of a non-convex function of a single variable. Each estimation of this function requires a linear regression (5) where the variables  $A$  and  $B$  are sampled along the 1-D contours  $\partial\Omega$ . The number of variables in this regression is thus small so that we decided to perform a brute force exhaustive search for  $q(\beta)$ . More advanced optimization schemes could be used as well to speed up the process. The final polynomial fit (6) only requires the resolution of a  $3 \times 3$  linear system.

## 5 Numerical Results

We benched the efficiency of our method on a synthetic model that is intended to be biologically plausible in term of both the spatial and temporal dynamics of the source.

**Signal model.** We generate a smooth source  $f_0$  as a space-time colored Gaussian noise. We restrict the support of the source by multiplying it with a smooth windowing function in order to obtain a compact support in

$\Omega \times [0, t_0]$  where  $t_0 = 40$ ,  $\Omega$  is a union of two disks of radius 0.08, centered at  $(0.5, 0.2)$  and  $(0.5, 0.7)$ .

The observation  $X = u + w$  with  $u = T_{\alpha_0}(f_0)$  is generated by using  $\alpha_0 = (a_0, b_0, c_0)$  with

$$a_0 = \frac{1}{s_0^2}, \quad b_0 = 2\frac{\rho_0}{s_0^2}, \quad c_0 = \left(\frac{\rho_0}{s_0}\right)^2$$

where  $s_0$  represent the biological speed of the propagating wave, and  $\rho_0$  accounts for the dissipation of the propagation. The noise  $w$  is a Gaussian white noise of standard deviation  $\sigma \|u\|_\infty$ , where  $\sigma \geq 0$  controls the strength of the noise. The wave propagation  $u$  is generated by solving numerically the (1) with semi-implicit finite difference scheme in time, spectral discretization of the spatial Laplacian, and absorbing boundary conditions using a perfect matched layer (PML) scheme. In the numerical experiments, we use  $s_0 = 1$  and  $\rho_0 = 1/10$  for a square domain of observations  $[0, 1]^2$  discretized using  $150 \times 150$  points on a uniform 2-D grid. Figure 2 shows a typical signal used for the numerical experiments.

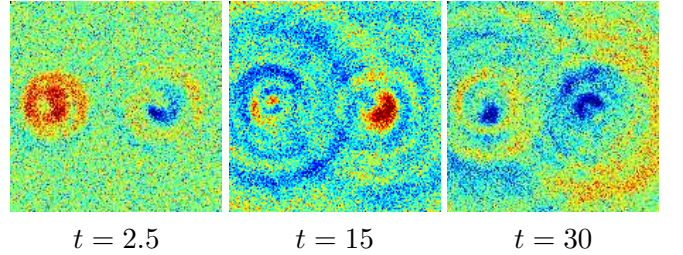


Figure 2: Example of synthetic signal  $X$  considered in our numerical experiment, here  $\sigma = 0.1$  (see Section 5).

**Numerical evaluation.** We measure the efficiency of our fitting procedure according to three noise level corresponding to  $\sigma = 0$  (no noise),  $\sigma = 0.03$  (low noise) and  $\sigma = 0.1$  (strong noise). We perform the fitting procedure described in Section 4 using  $\beta_{\max} = 0.5$  and  $|\Sigma| = 25$ .  $q(\beta)$  is computed for our shape parameter by solving (4) and then the polynomial fit  $\beta \mapsto a\beta^2 + b\beta + c$  is obtained by solving (6). After having computed the values for  $(a, b, c)$ , we estimate the relevant biological parameters (speed and dissipation) as  $s = \frac{1}{\sqrt{a}}$  and  $\rho = 2\frac{c}{b} \cdot q(\beta)$  is computed for 200 realizations of the noise  $w$ . Then we compute the relative error  $q_r(\beta) = \frac{q(\beta) - q_0(\beta)}{q_0(\beta)}$  for each realization. Figure 3 shows the expected value  $\mathbb{E}_\beta$  with respect to realizations of the noise  $w$  (resp. standard deviation  $\text{Std}_\beta$ ) of  $q_r(\beta)$  for  $0 \leq \beta \leq 2\beta_{\max}$ .

Table 5 shows statistics of speed  $s$  and dissipation  $\rho$  parameters. We observed in this table that estimation is not perfect in the noiseless case ( $\sigma = 0$ ) because of discretization error for both the signal generation and the

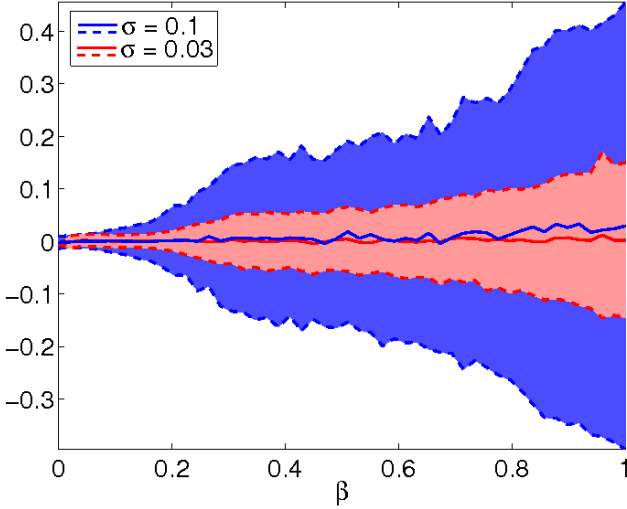


Figure 3: Display of the expected value  $\mathbb{E}_\beta$  (blue and red solid lines) of  $q_r(\beta)$ . The blue and red regions corresponds to confidence intervals defined as the set of  $(\beta, q)$  with  $|q - \mathbb{E}_\beta| \leq 2\text{Std}_\beta$ .

Table 1: Statistics of speed  $s$  and dissipation  $\rho$

	$\sigma$	Expected value	Std. Deviation
$\rho_0 = 0.1$	0	0.101	
	0.03	0.102	0.021
	0.1	0.125	0.14
$s_0 = 1$	0	0.99	
	0.03	1.001	0.026
	0.1	1.011	0.084

Laplace transform. Our method is able to estimate the value of  $s_0$  even in the presence of a reasonable noise. In the presence of a strong noise ( $\sigma = 0.1$ ), our method is more accurate for the estimation of the speed  $s_0$  than for the dissipation parameter  $\rho_0$ .

## 6 Conclusion and Perspectives

In this paper we have proposed a fast and robust method to estimate constant parameters in a linear PDE model using only a constraint on the (known) support of the sources. This method might be useful to calibrate biological models in computational neuroscience. We are currently working on the application of our method to real data from VSDOI experiments. This method is also quite general and might be extended to other settings, such as 3-D propagations.

**Acknowledgement.** We thank Laurent Demanet for his PML implementation of the wave equation solver. This work is supported by ANR grant NatImages (ANR-08-EMER-009) and FACETS (FET Bio-I3: 015879).

## References

- [1] N. Bleistein, J. K. Cohen, and J. W. Stockwell. *Multi-dimensional Seismic Imaging, Migration, and Inversion*. Springer Verlag, New York, 2001.
- [2] V. Bringuier, F. Chavane, L. Glaeser, and Y. Frégnac. Horizontal propagation of visual activity in the synaptic integration field of area 17 neurons. *Science*, 283:695–9, 1999.
- [3] A. Derode and Al. Recovering the green’s function from field-field correlations in an open scattering medium. *J Acoust Soc Am.*, 2003.
- [4] J. Garnier and G. Papanicolaou. Passive sensor imaging using cross correlations of noisy signals in a scattering medium. *SIAM J. Imaging Sciences*, 2:396–437, 2009.
- [5] A. Grinvald and R. Hildesheim. VSDI : A new era in functional imaging of cortical dynamics. *Nature Reviews Neuroscience*, 5(11), 2004.
- [6] Jerry M. Harris and Feng Yin. Nonlinear multi-frequency wave equation inversion. *SEG Technical Program Expanded Abstracts*, 13(1):988–991, 1994.
- [7] M. V. De Hoop and K. Solna. Estimating a green’s function from “field-field” correlations in a random medium. *SIAM Journal of Applied Mathematics*, 69(4):909–932, 2009.
- [8] D. Jancke, F. Chavane, S. Naaman, and A. Grinvald. Imaging cortical correlates of illusion in early visual cortex. *Nature*, 428:423–426, 2003.
- [9] P. E. Roland and Al. Cortical feedback depolarization waves: A mechanism of top-down influence on early visual areas. *PNAS*, 103(33):12586–12591, 2006.
- [10] N. Schmidt, G. Peyré, Y. Frégnac, and P. Roland. Separation of traveling waves in cortical networks using optical imaging. In *Proceedings of the 2010 IEEE international conference on Biomedical imaging: from nano to Macro*, ISBI’10, pages 868–871, Piscataway, NJ, USA, 2010. IEEE Press.
- [11] R. Snieder. Retrieving the green’s function of the diffusion equation from the response to a random forcing. *Phys. Rev. E*, 74(4):046620, Oct 2006.